Domain epitaxy: A unified paradigm for thin film growth

J. Narayan[a)]
Department of Materials Science and Engineering, North Carolina State University, Raleigh, North Carolina 27695-7916.

B. C. Larson
Solid State Division, Oak Ridge National Laboratory, Oak Ridge, Tennessee 37831

(Received 12 August 2002; accepted 21 October 2002)

We present a unified model for thin film epitaxy where single crystal films with small and large lattice misfits are grown by domain matching epitaxy (DME). The DME involves matching of lattice planes between the film and the substrate having similar crystal symmetry. In this framework, the conventional lattice matching epitaxy becomes a special case where a matching of lattice constants or the same planes is involved with a small misfit of less than 7%–8%. In large lattice mismatch systems, we show that epitaxial growth of thin films is possible by matching of domains where integral multiples of major lattice planes match across the interface. We illustrate this concept with atomic-level details in the TiN/Si(100) with 3/4 matching, the AlN/Si(100)with 4/5 matching, and the ZnO/$\alpha-Al_2O_3$(0001) with 6/7 matching of major planes across the film/substrate interface. By varying the domain size, which is equal to intregral multiple of lattice planes, in a periodic fashion, it is possible to accommodate additional misfit beyond perfect domain matching. Thus, we can potentially design epitaxial growth of films with any lattice misfit on a given substrate with atomically clean surfaces. *In situ* x-ray diffraction studies on initial stages of growth of ZnO films on sapphire correctly identify a compressive stress and a rapid relaxation within 1 to 2 monolayers, consistent with the DME framework and the fact that the critical thickness is less than 1 monolayer. DME examples ranging from the Ge–Si/Si(100) system with 49/50 matching (2% strain) to metal/Si systems with 1/2 matching (50% strain) are tabulated, strategies for growing strain-free films by engineering the misfit to be confined near the interface are presented, and the potential for epitaxial growth of films with any lattice misfit on a given substrate with atomically clean surfaces is discussed. © *2003 American Institute of Physics.* [DOI: 10.1063/1.1528301]

INTRODUCTION

Epitaxial growth of thin films and the control of defects in thin film heterostructures are key considerations for the next-generation of microelectronic, optical and magnetic devices.[1–3] As device feature sizes get smaller, single dislocations will have the ability to control device performance. In the well-established lattice-matching epitaxy, where the lattice misfit is small (less than 7%–8%), films grow pseudomorphically up to a ''critical thickness'' where it becomes energetically favorable for the film to contain dislocations.[4,5] In this case, the dislocations are generated at the film surface and glide to the interface; therefore, the Burgers vectors and planes of the dislocations are dictated by the slip vectors and glide planes of the crystal structure of the film.[6] On the other hand, for dislocations generated at the edge of islands during three-dimensional growth, geometrical constraints determine the Burgers vectors of the dislocations at the film–substrate interface. For example, during three-dimensional growth of germanium on silicon, it has been found that 90° dislocations with $a/2<110>$ Burgers vectors are created at the edge of germanium islands and lie in the (001) film–substrate interface.[7] Conventional wisdom maintains that lattice matching epitaxy during thin film growth is possible as long as the lattice misfit between the film and the substrate is less than 7%–8%. Smaller lattice misfit leads to smaller interfacial energy and coherent epitaxy is formed. Above this misfit, it was surmised that the film will grow textured or largely polycrystalline.[4,5]

In an earlier publication[8] and patent[9] we showed that films having a large misfit relative to the substrate ($>7\%-8\%$) grow epitaxially in the form of single crystals by domain matching epitaxy (DME), where integral multiples of lattice constants match across film–substrate interfaces.[8,9] Kwo *et al.*[10] reported epitaxial structures of Y and Gd films on Nb substrates via alignment of most densely packed rows between the film and the substrate ($[\bar{1}2\bar{1}0]=[002]$). However, the most densely packed row in the body-centered-cubic structure of niobium is [111] type not the [002]. When proposed, the DME concept represented a considerable departure from the conventional lattice matching epitaxy (LME) for thin film growth where films with misfit less than 7%–8% grow by one-to-one matching of lattice constants across the film–substrate interface. In the present work, the original concept of DME has been generalized. In the present DME, integral multiples of lattice planes match across the film–substrate interface, and the size of the domain equals integral multiples of planar spacing. If the film and the substrate have similar crystal structures, then the matching of planes (present DME) becomes equivalent to the matching of lattice constants (earlier DME patent.[9] Accordingly, for small

[a)]Author to whom correspondence should be addressed; electronic mail: j_narayan@ncsu.edu

 © 2003 American Institute of Physics

Downloaded 04 Sep 2009 to 160.91.157.167. Redistribution subject to AIP license or copyright; see http://jap.aip.org/jap/copyright.jsp

misfits ($<7\%-8\%$), the generalized DME is equivalent to the conventional LME. In our earlier work, we showed that TiN can grow epitaxially on a silicon substrate with about 22% lattice misfit via domain matching epitaxy where four lattice constants of TiN matched with roughly three of silicon across the film–substrate interface.[8,9] Simple theoretical modeling suggested that the DME led to a gain in the total energy.[11] Since the initial DME report, many systems with a large misfit have been grown with a remarkable success.[12–16] However, atomistic details, such as the relaxation process, the nature of dislocations in such systems, and the relation between DME and LME have not been clarified.

We illustrate domain matching epitaxy in TiN/Si(100), AlN(0001)/Si(111), and ZnO/αAl_2O_3(0001) systems, which contain misfits slightly off perfect 3/4, 5/4, and 6/7 matching, respectively. Each of these systems has its unique characteristics and importance. The TiN/Si(100) represents cube-on-cube epitaxy, where there is equivalence between the matching of planes and lattice constants. However, since TiN has a sodium chloride structure ($Fm3m$) compared to silicon's diamond cubic lattice ($Fd3m$), there are subtle differences, such as {110} dislocation glide planes in TiN versus {111} glide planes in silicon. The next example is AlN(0001)/Si(111), where the sixfold symmetry in the basal (0001) plane of the hexagonal wurtzite AlN structure ($P63mc$) matches the threefold symmetry of the silicon (111) plane. In this system domain matching occurs without any rotation in the basal plane. The third example involves epitaxial growth of hexagonal wurtzite structure ($P63mc$) ZnO on saphhire with rhombohedral (hexagonal, $R-3c$) structure in the basal plane. In this case, there is a 30° or 90° rotation in the basal plane, which is similar to III–nitride growth rotation on the (0001) plane of sapphire.

The primary focus of the research presented here is on systems with misfits slightly off perfect one-to-one domain (integral) matching. We show that additional misfit can be accommodated by changing the domain size within the DME framework. A careful examination of grain boundary structure shows that the additional tilt in the boundary can be accommodated by changing the periodicity of dislocations in the boundary. This is consistent with the concept of domain size variation. Thus, it is possible to grow epitaxial films with any lattice misfit just as it is possible to have grain boundaries of any tilt.[17,18] An important feature of the domain epitaxy concept in that most of the strain is relieved quickly within a couple of monolayers, so that the misfit strain can be engineered and confined near the interface. This makes it possible for the rest of the film to be grown free of defects and lattice strains. This is specifically illustrated for the ZnO/αAl_2O_3 system using transmission electron microscopy (TEM) studies and *in situ* x-ray diffraction measurements using a synchrotron x-ray source. This feature of the domain matching epitaxy growth process may provide a critical advantage over small-misfit lattice matching epitaxy, where most of the dislocations are generated on the surface, beyond the critical thickness, and then the dislocations glide to the interface as half loops. The half-loop glide process leads to the formation of detrimental threading dislocations throughout the electrically active regions of the film. The nature of dislocations (specifically lattice planes and Burgers vectors) within the DME framework is dictated by geometrical constraints of the growth process; this is in contrast to the LME process, where the Burgers vectors and the planes of the dislocations generated via deformation are normal slip vectors.

FUNDAMENTAL CONSIDERATIONS IN LME AND DME

In the domain matching epitaxy, we consider the matching of lattice planes, which could be different in different directions of the film–substrate interface. In the DME framework, the film can have either a fixed or the same orientation relationship with the substrate, depending upon the nature of the misfit. The misfit is accommodated by matching of integral multiples of lattice planes, and there is one extra half plane (dislocation) corresponding to each domain. The misfit can range from being very small to very large. In the small misfit regime, the DME reduces to LME where matching of the same planes or lattice constants is considered with a misfit typically less that 7%–8%. If the misfit falls in between the perfect matching ratios of planes, then the size of the domain can vary in a systematic way to accommodate the additional misfit. In the conventional LME, the initial or unrelaxed misfit strain is (ε_c) is given by $\varepsilon_c = a_f/a_s - 1$, where a_f and a_s are lattice constant of the film and the substrate, respectively. In LME, the ε_c is less than 7%–8% which is relaxed by the introduction of dislocations beyond the critical thickness during thin film growth. In the domain matching epitaxy, the matching of lattice planes of the film d_f with those of the substrate d_s is considered with similar crystal symmetry. In DME, the film and the substrate planes could be quite different as long as they maintain the crystal symmetry. The LME, on the other hand, involves the matching of the same planes between the film and the substrate. In DME, the initial misfit strain ($\varepsilon = d_f/d_s - 1$) could be very large, but this can be relaxed by matching of m planes of the film with n of the substrate. This matching of integral multiples of lattice planes leaves a residual strain of ε_r given by

$$\varepsilon_r = (md_f/nd_s - 1), \tag{1}$$

where m and n are simple integers. In the case of a perfect matching $md_f = nd_s$, and the residual strain ε_r is zero. If ε_r is finite, then two domains may alternate with a certain frequency to provide for a perfect matching according to

$$(m+\alpha)d_f = (n+\alpha)d_s, \tag{2}$$

where α is the frequency factor, for example, if $\alpha = 0.5$, then m/n and $(m+1)/(n+1)$ domains alternate with an equal frequency.

Assuming $d_f > ds$, we have $n > m$. Therefore,

$$n - m = 1 \text{ or } f(m). \tag{3}$$

The difference between n and m could be 1 or some function of m. In Fig. 1, $n-m=1$ for $\varepsilon = 0\% - 50\%$ and $n-m = f(m)$ for $\varepsilon = 50\% - 100\%$.

From Eqs. (1) – (3), we can derive

$$(m+\alpha)\,\varepsilon = 1 \text{ or } f(m). \tag{4}$$

Downloaded 04 Sep 2009 to 160.91.157.167. Redistribution subject to AIP license or copyright; see http://jap.aip.org/jap/copyright.jsp

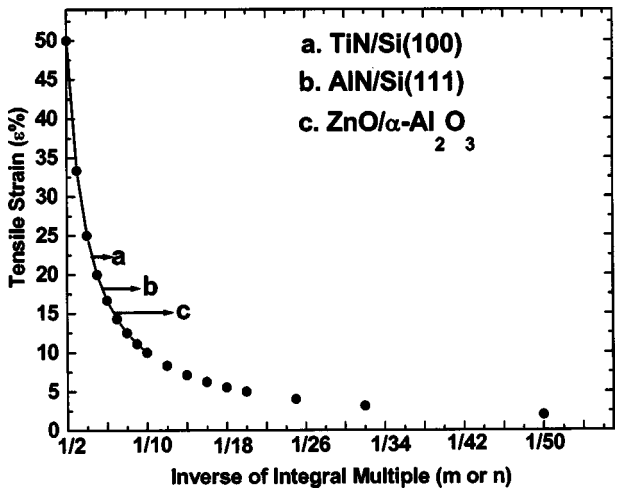

FIG. 1. Unified plot of strain vs film–substrate planar spacing ratio. The LME region is above about 12/13 ratio or below about 7.7% strain.

Equation (4) basically governs the domain epitaxy, as plotted in Fig. 1. The basic assumption in our simple model is that there is a complete relaxation of the strain without any dislocation nucleation barrier, which is borne out by our *in situ* x-ray diffraction measurements. Figure 1 shows a general plot of misfit percent strain as a function of inverse of integral multiple of planes matching across the interface. It should be noted that a 45° rotation in some cubic systems such as $SrTiO_3/GaAs(100)$, involves matching of {200} and {220} planes of the film and the substrate, respectively.Table I provides a summary of different systems which have been grown with various misfit strains. The table also includes the systems which fall in between the two domains where two domains alternate with a periodicity needed for a complete relaxation. The plot in Fig. 1 provides a unified framework of lattice matching and domain matching epitaxy with misfit strain ranging from 2% to 50% (50% corresponding to 1/2 matching). If the domain matching is not perfect, epitaxy occurs by accommodating the additional misfit by changing the domain size, controlled by the parameter α. In this framework, it is important to realize that the nature of the dislocations remains the same, only their periodicity changes. This domain variation concept can also be extended to the dislocation model of grain boundaries. The experimental results (in Fig. 2) on the dislocation structure of a (100) tilt boundary in the $YBa_2Cu_3O_{7-\delta}$ superconductor show that a periodic variation in dislocation spacing of $a[010]$ Burgers vectors (between 9 and 10), in fact, accommodates the additional tilt. The tilt boundary angle of 5.9° is accommodated by a periodic variation of 9 and 10 of (100) planes, corresponding to 5.6° and 6.3°, respectively. This concept is quite significant in terms of predicting the nature of dislocations at the interfaces in both cases. These points will become clearer as we discuss specific cases of domain matching epitaxy and the nature of dislocations, including their periodicity.

TABLE I. Domain epitaxy for thin film growth.

m/n	Planar spacing ratio	Experimental examples	Strain ε%
1/10	0.1		90.0%
1/9	0.11		88.8%
1/8	0.125		87.5%
1/7	0.143		85.7%
1/6	0.166		83.3%
1/5	0.20		80.0%
1/4	0.25		75.0%
1/3	0.33		66.7%
1/2 and 1/3	0.33–0.50	Mo, Nb, Ta, W/Si; Ni_3Al/Si(100)	50.0%
1/2	0.50	Fe/Si, Cr/Si, NiAl//Si(100)	
2/3	0.666	Cu/Si(100)	33.33%
3/4	0.750	TiN/Si(100)	25.00%
4/5	0.80	AlN/Si(111)	20.00%
5/6	0.83	$\alpha-Al_2O_3$/ZnO(0001)	16.67%
6/7	0.857	$\alpha-Al_2O_3$/ZnO(0001), Cu/TiN(100)	14.29%
7/8	0.8750	$\alpha-Al_2O_3$/GaN(0001)	12.50%
8/9	0.888	$\alpha-Al_2O_3$/AlN(0001),	11.11%
9/10	0.90	$YBa_2Cu_3O_{7-}\delta$/MgO(001)	10.0%
11/12	0.9166	$YBa_2Cu_3O_{7-}\delta$/MgO(001)	8.33%
12/13	0.9230	STO/MgO(001)	7.69%
13/14	0.3286		7.14%
14/15	0.9333		6.67%
16/17	0.9412		5.88%
17/18	0.9444		5.55%
18/19	0.9474		5.26%
19/20	0.9500		5.00%
20/21	0.9524		4.76%
22/23	0.9556		4.35%
24/25	0.96	Ge/Si(100)	4.0%
31/32	0.9687		3.13%
49/50	0.98	Ge–Si/Si(100)	2.0%

Downloaded 04 Sep 2009 to 160.91.157.167. Redistribution subject to AIP license or copyright; see http://jap.aip.org/jap/copyright.jsp

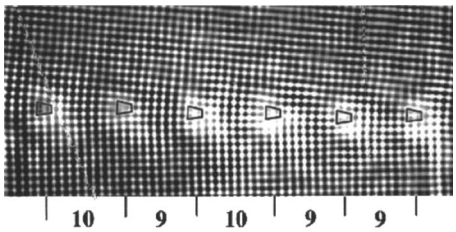

FIG. 2. Small-angle (100) tilt boundary in $YBa_2Cu_3O_{7-\delta}$ with angle ($\theta = 5.9°$), where dislocations with a [100] Burgers vectors alternate with a frequency of 9 and 10 spacing of (100) planes to accommodate this tilt.

TiN/Si(100) SYSTEM

Epitaxial growth of TiN on the silicon substrate represents a major milestone for next-generation semiconductor devices for direct ohmic contacts as well as for diffusion barriers in copper metallization. However, with a misfit of over 22% for cube-on-cube TiN ($a = 0.424$ nm) epitaxy over silicon ($a = 0.543$ nm), it is beyond the critical strain (7%–8%) of conventional lattice matching. However, epitaxial growth of TiN on silicon substrate was demonstrated by the concept of domain matching epitaxy. The films were grown using a standard pulsed laser deposition method described in Ref. 8. Figure 3 shows a detailed high-resolution cross-section TEM micrograph, where 3/4 and 4/5 domains alternate. The high-resolution TEM micrograph was taken in the <110> zone axis of Si and TiN, showing the atomic structure of the Si/TiN interface and the dislocations associated with it. The corresponding diffraction pattern (shown in the inset) confirms cube-on-cube domain epitaxy for this system. It is interesting to note the matching of {111} extra half planes in silicon as well as TiN. The implications of these on the nature of dislocations will be discussed later in the section. From Fig. 1, the lattice misfit of 22% lies in the middle 3/4 and 4/5 matching, which explains the alternating of domains. In fact with $\alpha = 0.5$ [Eq. (2)], $3.5a_{Si} = 19.01$ matches quite well with $4.5 \times a_{TiN} = 19.08$, which also represents the size of domain for the system with virtually no residual misfit. In our earlier study, we considered various energy terms for epitaxial growth of TiN on Si(100) and found a significant reduction in energy due to domain matching epitaxy compared to the unrelaxed state.[11]

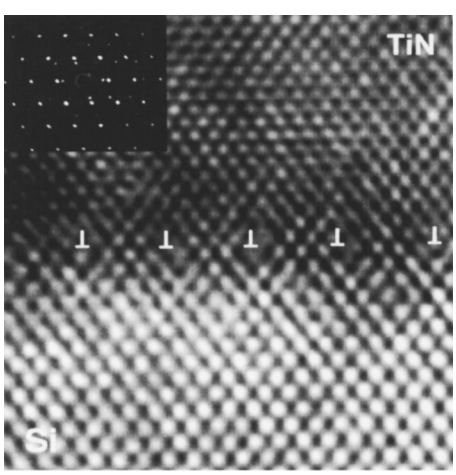

FIG. 3. (a) High-resolution cross-section in <110> direction from the TiN/Si(100) system, showing domain matching of TiN with silicon. Here the frequency factor ($\alpha = 0.5$) for 3/4 and 4/5 domains. The $a/2<110>$ misfit dislocations lie in {111} planes in both TiN and silicon; the inset shows a corresponding <110> TiN/Si diffraction pattern.

The nature of dislocations can be established directly from the high-resolution TEM micrographs. The Burgers vector of the dislocations is determined to be $a/2<110>$ lying in {111} planes. The two sets of $a/2<110>$ dislocations combine at the interface to produce $a/2<110>$ dislocations lying in the {001} interfaces. This dislocation reaction can be described as: $a/2[101](11\bar{1}) + a/2[01\bar{1}](111) \rightarrow a/2[110](001)$. In some cases, the dislocations do not combine and thus create an extended core structure associated with the pair of dislocations. The formation of $a/2<110>$ dislocations in the {111} plane in TiN with a sodium chloride structure represents a significant finding. The TiN having a sodium chloride structure has {110} slip planes with $a/2<110>$ Burgers vectors. Only under certain extreme nonequilibrium conditions such as high fields, $a/2<110>$ have dislocations lying in {001} planes been observed.[19] However, this is first for the $a/2<110>$ dislocation in {111} planes of sodium chloride structure. These dislocations or slip systems may impact mechanical and physical properties of TiN films or materials of sodium chloride structure, in general, in a significant way. According to the von Mises criterion, five independent slip systems are needed for a crystal to undergo a general plastic deformation by slip. In TiN having a sodium chloride structure, there are only two independent $a/2<110>\{110\}$ slip systems available, which restricts a general deformation, resulting in twinning and fracture. However, with $a/2<110>\{110\}$ slip systems, there are 384 ways of choosing five independent slip systems, which can lead to a general deformation of TiN.[20]

III–NITRIDE EPITAXY ON SI(111)

Epitaxial growth of III–nitrides having a wurtzite structure on silicon (111) substrates are needed as a template to grow GaInN and AlGaInN alloys as well as to integrate III–nitride based optoelectronic devices with microelectronic devices. Additionally, AlN has a high thermal conductivity (320 W/M K), high thermal stability (up to 2200 °C), high resistivity ($10^{13}\,\Omega$ cm), high dielectric strength (14 kV/cm), and high chemical inertness. The hardness and thermal expansion coefficient (2.56×10^{-6}/K) are comparable to that of silicon. These properties make AlN an ideal candidate for application in microelectronic to optoelectronics including high-temperature devices and electronics packaging.[21,22]

Epitaxial growth of AlN (0001) with hexagonal wurtzite structure ($a = 3.11$ A, $c = 4.982$ A) on silicon (111) substrate occurs via matching of four silicon (220) planes with five $(2\bar{1}\bar{1}0)$ planes of AlN. The spacing of $(2\bar{1}\bar{1}0)$ AlN planes ($a/2 = 1.556$ A) result is close to 19% strain with (220) planes of silicon. Using this strain, we found that (from Fig. 1), 5 AlN $(2\bar{1}\bar{1}0)$/4(220) matching results in less than 1% residual strain. Figure 4(a) shows a cross-section TEM micrograph where the alignment of $(2\bar{1}\bar{1}0)$ planes of AlN with (220) planes of silicon is clearly delineated. This alignment

Downloaded 04 Sep 2009 to 160.91.157.167. Redistribution subject to AIP license or copyright; see http://jap.aip.org/jap/copyright.jsp

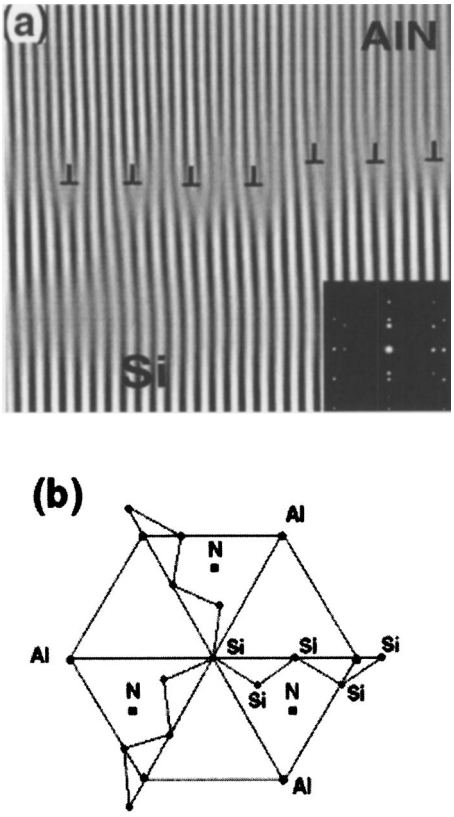

FIG. 4. (a) Domain epitaxy in the AlN/Si(111) system, $(01\bar{1}0)$AlN, and $(11\bar{2})$Si in high-resolution cross section showing the matching of AlN$(2\bar{1}\bar{1}0)$ and Si(220)planes with $\alpha=0.25$ for 4/5 and 5/6 domains, corresponding (inset) diffraction pattern shows the alignment AlN and Si planes; and b) schematic of arrangement of atoms in the basal plane of AlN and Si(111).

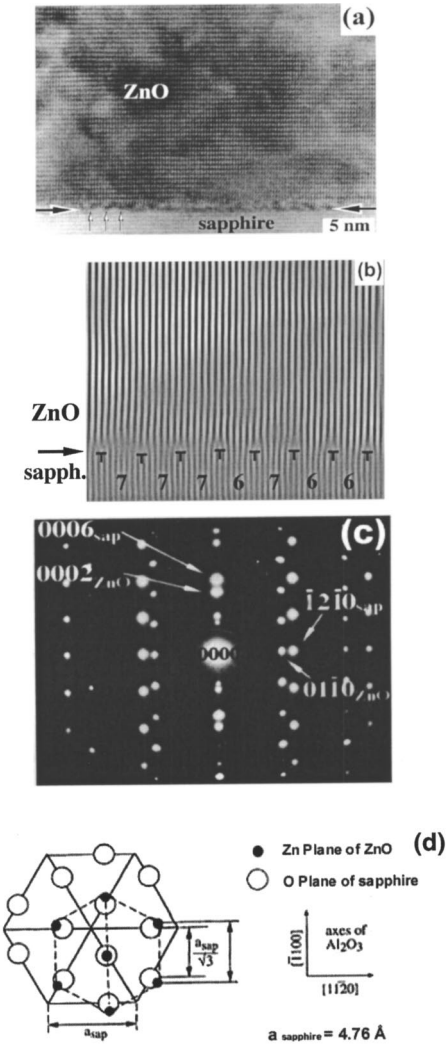

FIG. 5. (a) High resolution TEM cross section with $(01\bar{1}0)$ foil plane of sapphire and $(2\bar{1}\bar{1}.0)$ plane of ZnO showing domain epitaxy in ZnO/α Al_2O_3 (sapphire) system; (b) Fourier-filtered image of matching of $(2\bar{1}\bar{1}0)$ ZnO and $(30\bar{3}0)$ sapphire planes with a frequency factor ($\alpha=0.5$) for 5/6 and 6/7 domains; (c) corresponding electron diffraction pattern showing the alignment of planes in ZnO and sapphire; and (d) schematic of arrangement of atoms in the basal plane of ZnO and sapphire.

is confirmed by the corresponding diffraction pattern shown in the inset. The (111) planes of the silicon substrate are shown schematically in Fig. 4(b) on which basal planes of AlN {0001} grow with the *a* axis of AlN $[2\bar{1}\bar{1}0]$ aligned with the [220] direction of silicon. In this field of view, five planes of AlN clearly match four planes of silicon with one exception where six planes of AlN match five planes of silicon. This is predicted from our master diagram in Fig. 1 for a 19% strain. The perfect matching is predicted from Eq. (3) for $\alpha=0.25$. Thus, the deviations from the ideal 5/4 matching (corresponding to 20% strain) are accommodated by variation in domain size, rather than an additional set of secondary dislocations to relieve the difference in the strain from the ideal 5/4 matching.

DOMAIN EPITAXY OF ZnO AND III-NITRIDES ON $\alpha-Al_2O_3(0001)$

There is a growing interest in growing high quality thin films of ZnO and its alloys for light emitting diodes (LEDs) and laser diodes (LDs) applications. The bandgap of ZnO can be tuned by alloying with MgO (8.0 eV, upshift) or with CdO (1.9 eV, downshift). The ZnO can also be used as a template for III–nitride growth separately as well as on on sapphire substrates. Therefore, the growth of high quality ZnO (having wurtzite hexagonal structure, $a=3.252$ A, $c=5.213$ A) on a practical substrate such as sapphire ($a=4.758$ A, $c=12.991$ A) presents a major challenge. The growth of systems with such a large misfit is possible only with domain matching epitaxy, where the misfit can be accommodated by the matching of planes.[15,23]

Figure 5(a) shows a high-resolution cross-section TEM micrograph where the ZnO film plane is $(2\bar{1}\bar{1}0)$ and the sapphire substrate is $(01\bar{1}0)$. The epitaxial growth of ZnO film with an atomically sharp interface is clearly demonstrated. The Fourier-filtered image in Fig. 5(b) clearly delineates the matching of 5 or 6 $(2\bar{1}\bar{1}0)$ planes of ZnO with 6 or 7 $(30\bar{3}0)$ planes of sapphire. The corresponding diffraction pattern, which confirms this alignment of planes, is shown in Fig. 5(c). The *c* plane of ZnO rotates by 30° in the basal *c* plane of sapphire as shown in Fig. 5(d), which leads to alignment of 1/2 $(30\bar{3}0)$ planes of sapphire with $(2\bar{1}\bar{1}0)$ planes or

Downloaded 04 Sep 2009 to 160.91.157.167. Redistribution subject to AIP license or copyright; see http://jap.aip.org/jap/copyright.jsp

a planes of the ZnO film. Thus, we are looking at domain matching of sapphire planes (having $a_{sap}/\sqrt{3}$ spacing) with *a* planes of ZnO. By alternating the domains, there is almost a perfect matching as $5.5\times a_{ZnO}$ (3.2536 A)$\approx 6.5\,\alpha-Al_2O_3$ (2.7512 A), as predicted for $\alpha=0.5$ from Eq. (3). These numbers include planar spacings at the growth temperature, taking into account the respective coefficients of thermal expansion. From the planar spacing, we calculate a strain of 15.44%, which falls in between 5/6 and 6/7 matching in the master plot of Fig. 1. This is in complete agreement with experimental observation of Figs. 5(a) and 5(b).

IN-SITU X-RAY DIFFRACTION MEASUREMENTS

The details of lattice relaxation process during initial stages of ZnO growth on sapphire ($\alpha-Al_2O_3$), (0001) substrates have been studied by *in situ* x-ray diffraction study using the UNI-CAT undulator beam line at the Advanced Photon Source. In these experiments, the laser-ablation, film-growth chamber[24,25] is mounted on a so-called 2+2 x-ray diffractometer where surface scattering measurements in specular and off-specular directions were made to investigate the details of initial stages of thin film growth. Time-slice x-ray crystal truncation rod (CTR) measurements made after each excimer laser ablation pulse revealed the surface structure transients associated with ZnO clustering and crystallization to last about 2 s following the abrupt $\sim 5\ \mu$s duration of laser deposition.

Specular CTR anti-Bragg measurements at the sapphire (0 0 5/2) position showed only one well-defined growth oscillation, indicating three-dimensional (3D) growth rather than layer by laser growth. Off-specular CTR measurements along the $(H, 0, -H, 0.3)$ direction showed thermally activated relaxation of the 15.44% lattice mismatch between ZnO and Al_2O_3 along with a 30° in-plane rotation around the *c* axis. As shown in Fig. 6, a broad, nearly relaxed ZnO in-plane diffraction peak appears after the deposition of 3 monolayers at 400 °C ($\sim$25 pulses/monolayer), while a sharper and more fully relaxed ZnO peak appears after only 2 monolayers at 585 °C. The peak after 150 pulses at 585 °C occurs at $H=0.845$ corresponding to the fully relaxed ZnO film. Subsequent measurements (not plotted here) showed that incommensuration occurs within the first layer of the deposition, and the nature of the strain is compressive as expected for matching of *a* planes of of ZnO (spacing 3.2536 A) with underlying sapphire planes (2.7512 A). These results clearly established a rapid relaxation of ZnO films on sapphire. The relaxation process was found to be thermally activated because the ZnO thickness corresponding to full relaxation decreased as the deposition temperature increased.[24] The relaxation process requires the creation of dislocations, which involves nucleation and propagation of dislocations. Both of these steps are thermally activated. The nucleation barrier can be partially overcome by the surface steps,[26] and the propagation is very small in DME due to the proximity of the interface.

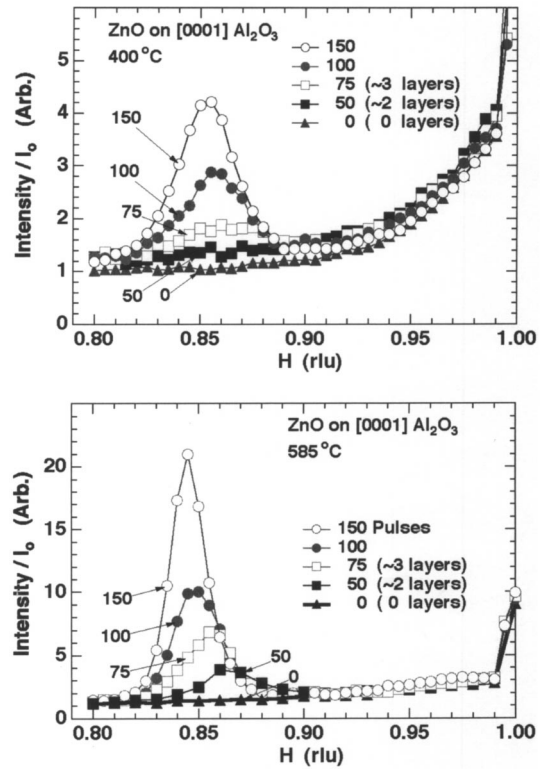

FIG. 6. X-ray surface diffraction measurements along the $(H, 0, -H, 0.3)$ direction showing the growth of ZnO films on sapphire with sapphire in-plane lattice parameter approaching $H=0.845$ corresponding to a fully relaxed position after a few monolayers.

LATTICE RELAXATION AND DEFECT REDUCTION PROCESSES

The rapid relaxation process in DME is consistent with the fact that the critical thickness under these large misfits is less than 1 monolayer.[26] As a result, dislocations can nucleate during initial stages of growth and confine most of the defects near the interface, leading to fewer defects in the active region of the device. Figures 7(a) and 7(b) show TEM cross-section images of ZnO/saphhire specimens under two

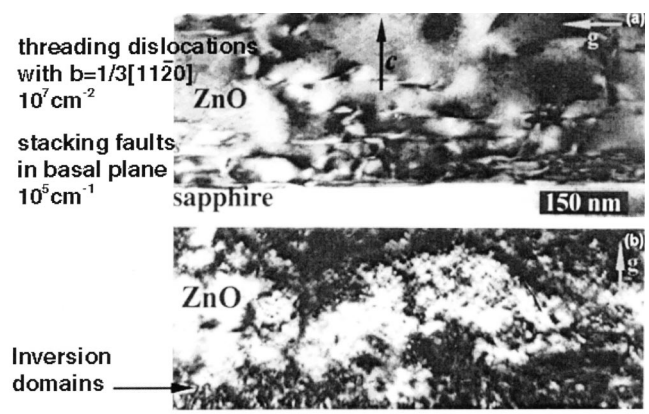

FIG. 7. Cross section TEM micrograph of ZnO/ sapphire specimens under two different diffraction conditions ($\bar{g}$ vectors) showing a low density of threading dislocations, stacking faults and domain boundaries. Most of the dislocations are confined to the interface.

Downloaded 04 Sep 2009 to 160.91.157.167. Redistribution subject to AIP license or copyright; see http://jap.aip.org/jap/copyright.jsp

different diffraction conditions to image dislocations. The ZnO films were grown by pulsed laser deposition at 790 °C. From these micrographs, the density of threading dislocations with Burgers vector $b=1/3[11\bar{2}0]$ was estimated to be $10^7\,\mathrm{cm}^{-2}$, which is 3 orders of magnitude lower than normally observed for the misfit of this magnitude (15.44%). The density of stacking faults (planar defects) was estimated to be $10^5\,\mathrm{cm}^{-1}$. It is interesting to note that most of the dislocations and other defects (stacking faults and domain boundaries) are confined to the ZnO/sapphire interface as expected from the domain epitaxy growth.

Since the critical thickness at which it becomes energetically feasible for the film to contain dislocations is less than 1 monolayer, the dislocations nucleate at free-surface steps within 1 monolayer and locate at the interface where there is an energy minimum. An important consideration here is a large number density of surface steps within the monolayer, which can provide easy nucleation sites for dislocations. If the initial growth is 2D, the dislocations can propagate throughout the entire length of the film, and confine themselves near the interface without creating threading dislocations. However, if the initial growth is a mixture of 2D and 3D growth then dislocation segments may not propagate throughout the entire length and threading segments may ensue. Depending upon the nature of growth characteristics and the number density of surface steps, this characteristic of DME may be used to reduce the number density of threading dislocations and confine most of the misfit dislocations near the interface.

On the other hand, if the critical thickness is large as in a low-misfit system, then the dislocations nucleate at the free-surface steps and then glide to the interface. The process creates a half-loop configuration with two threading segments and a straight segment along the interface. Since there is a nucleation barrier for the dislocation, misfit is not fully relaxed.[26] In addition, threading segments do not expand to the edges due to the presence of other dislocations and obstacles, and as a result a high-density of these dislocations is retained within the film. Since these dislocations are purely glide or slip dislocations, their planes and Burgers are controlled by the slip systems of the film. The relaxation process in low misfit systems is gradual due to this nucleation barrier, leading to a large number of threading dislocations. Thus, in the DME framework, the films having larger misfits can be grown with fewer defects in the active region.

CONCLUSION

We have provided the concept of domain epitaxy for thin film growth having a small as well as large misfit strain with the substrate. We have shown that by matching integral multiples of major planes between the film and the substrate, it is possible to grow films with small as well as large misfits. We have discovered that systematic variations in domain sizes are created to accommodate misfits that fall between the integral multiples. As the domain size changes, the nature of the dislocations remains the same. For large misfit strains, the critical thickness is less than 1 to 2 monolayers, so dislocations corresponding to full lattice relaxation are generated at or within 1 monolayer of the interface; and the remainder of the film can be grown virtually strain and misfit-dislocation free. Thus, the DME concept can be used to engineer and confine misfit strains near the interface, and films with larger misfits can be grown with a fewer number of defects in the active regions, compared to the films with smaller misfits grown by LME. We have recently shown that the number density of dislocations can be reduced considerably by utilizing a two-step growth procedure for large mismatch systems. In the first step, 1–2 monolayers are grown and given time for all the dislocations to be formed corresponding to full lattice relaxation. Then, in the second step, the film is grown virtually strain free with a substantially lower density of threading dislocations. The nature of misfit dislocations in terms of Burgers vectors and habit planes are determined by geometrical constraints, rather than by deformation in the normal slip systems. This is similar to the observations of unusual dislocation structures at the grain boundaries formed as a result of geometrical constraints. The formation of $a/2<100>$ dislocations in {111} planes in TiN has been shown to be a result of geometrical constraints during domain epitaxy on the Si(100) substrate. Thus, domain epitaxy provides a mechanism to grow epitaxial films on substrates with large misfits, and opens a new frontier in next-generation solid state technology.

ACKNOWLEDGMENTS

The authors are pleased to acknowledge useful discussions with Dr. Haiyan Wang, Dr. John Budai, and Professor John Hirth; the contributions of Mirang Yoon, Jon Tischler, Gyula Eres, Doug Lowndes, Paul Zschack, and John Budai on the pulsed-laser deposition ZnO growth experiments at the Advanced Photon Source are gratefully acknowledged. This research was supported in part by the National Science Foundation and in part by the Division of Materials Sciences, U.S. Department of Energy under Contract No. DE-AC05-00OR22725 with UT-Battelle, LLC. UNICAT is supported by the University of Illinois, Material Research Lab., Oak Ridge National Laboratory, National Institute for Standards and Technology, and UOP, Inc. Use of the Advanced Photon Source was supported by the U.S. Department of Energy, Office of Science, Office of Basic Energy Sciences, under Contract No. W-31-109-ENG-38.

[1] H. J. Queisser and E. E. Haller, Science **281**, 945 (1998).
[2] S. Nakamura, Science **281**, 956 (1998).
[3] S. Mahajan, Acta Mater. **48**, 137 (2000).
[4] J. W. Mathews and A. E. Blakeslee, J. Cryst. Growth **27**, 188 (1974).
[5] J. W. Mathews, Epitaxial Growth, Part B, Materials Science Series 560 (Academic, New York, 1975).
[6] J. Narayan and S. Sharan, Mater. Sci. Eng., B **10**, 261 (1991).
[7] F. K. LeGoues, M. C. Reuter, J. Tersoff, M. Hammer, and R. M. Tromp, Phys. Rev. Lett. **73**, 300 (1994).
[8] J. Narayan, P. Tiwari, X. Chen, R. Chowdhury, and T. Zheleva, Appl. Phys. Lett. **61**, 1290 (1992).
[9] J. Narayan, U.S. Patent No. 5,406,123 (April 11, 1995).
[10] J. Kwo. M. Hong, and S. Nakahara, J. Appl. Phys. **49**, 319 (1986).
[11] T. Zheleva, K. Jagannadham, and J. Narayan, J. Appl. Phys. **75**, 860 (1994).
[12] R. D. Vispute, R. Chandhury, P. Tiwari, and J. Narayan, Appl. Phys. Lett. **65**, 2565 (1994).
[13] R. D. Vispute, H. Wu, and J. Narayan, Appl. Phys. Lett. **67**, 1549 (1995).

Downloaded 04 Sep 2009 to 160.91.157.167. Redistribution subject to AIP license or copyright; see http://jap.aip.org/jap/copyright.jsp

[14] R. D. Vispute, J. Narayan, and J. D. Budai, J. Appl. Phys. **80**, 6720 (1996).
[15] J. Narayan, K. Dovidenko, A. Sharma, and S. Oktyabrsky, J. Appl. Phys. **84**, 2597 (1998).
[16] A. K. Sharma, J. Narayan, C. Jin, A. Kvit, S. Chattopadhyay, and C. B. Lee, Appl. Phys. Lett. **76**, 1458 (2000).
[17] S. Okytyabrsky, K. Kalyanraman, K. Jagannadham, and J. Narayan, J. Mater. Res. **14**, 2764 (1999).
[18] J.-M. Penisson, in *Interface Science and Engineering*, edited by R. Raj and S.L. Sass, J. Phys. (Paris), Colloq. **C5**, 87 (1988).
[19] J. Narayan, J. Appl. Phys. **37**, 2703 (1985).
[20] J. P. Hirth and J. Lothe, *Theory of Dislocations* (Wiley, New York, 1998).
[21] S. Strite and H. Morkoc, J. Vac. Sci. Technol. B **10**, 1237 (1992).
[22] S. C. Jain, M. Willander, J. Narayan, and R. Van Overstraeten, J. Appl. Phys. **87**, 965 (2000).
[23] J. Narayan, A. K. Sharma, A. Kvit, C. Jin, J.F. Muth, and O. W. Holland, Solid State Commun. **121**, 9 (2002).
[24] J. Z. Tischler, G. Eres, M. Yoon, B. C. Larson, D. H. Lowndes, J. D. Budai, and P. Zschack, Ref. No. ORNL-6964, 1999.
[25] G. Eres, J. Z. Tischler, M. Yoon, B. C. Larson, C.M. Rouleau, D.H. Lowndes, and P. Zschack, Appl. Phys. Lett. **80**, 3379 (2002).
[26] M. Ichimura and J. Narayan, Philos. Mag. A **72**, 297 (1995).

Downloaded 04 Sep 2009 to 160.91.157.167. Redistribution subject to AIP license or copyright; see http://jap.aip.org/jap/copyright.jsp